Molecular & Biochemical Parasitology 225 (2018) 84–93

Contents lists available at ScienceDirect

Molecular & Biochemical Parasitology

journal homepage: www.elsevier.com/locate/molbiopara

TbUTP10, a protein involved in early stages of pre-18S rRNA processing in *Trypanosoma brucei*

Drahomíra Faktorová[a,b,*], Anita Bär[b,1], Hassan Hashimi[a,b], Katherine McKenney[c,d], Aleš Horák[a,b], Achim Schnaufer[e], Mary Anne T. Rubio[c,d], Juan D. Alfonzo[c,d,f], Julius Lukeš[a,b,*]

[a] Institute of Parasitology, Biology Centre, Czech Academy of Sciences, 37005, České Budějovice (Budweis), Czech Republic
[b] Faculty of Sciences, University of South Bohemia, 37005, České Budějovice, Czech Republic
[c] Department of Microbiology, The Ohio State University, Columbus, OH, USA
[d] The Center for RNA Biology, The Ohio State University, Columbus, OH, USA
[e] Centre of Immunity, Infection and Evolution and Institute of Immunology & Infection Research, University of Edinburgh, Edinburgh, United Kingdom
[f] The Ohio State Biochemistry Program, The Ohio State University, Columbus, OH, USA

ARTICLE INFO

Keywords:
Trypanosoma
Ribosomal RNA
Pre-18S rRNA processing
UTP10
U3 snoRNA

ABSTRACT

Ribosome biosynthesis, best studied in opisthokonts, is a highly complex process involving numerous protein and RNA factors. Yet, very little is known about the early stages of pre-18S rRNA processing even in these model organisms, let alone the conservation of this mechanism in other eukaryotes. Here we extend our knowledge of this process by identifying and characterizing the essential protein TbUTP10, a homolog of yeast U3 small nucleolar RNA-associated protein 10 - UTP10 (HEATR1 in human), in the excavate parasitic protist *Trypanosoma brucei*. We show that TbUTP10 localizes to the nucleolus and that its ablation by RNAi knock-down in two different *T. brucei* life cycle stages results in similar phenotypes: a disruption of pre-18S rRNA processing, exemplified by the accumulation of rRNA precursors, a reduction of mature 18S rRNA, and also a decrease in the level of U3 snoRNA. Moreover, polysome profiles of the RNAi-induced knock-down cells show a complete disappearance of the 40S ribosomal subunit, and a prominent accumulation of the 60S large ribosomal subunit, reflecting impaired ribosome assembly. Thus, TbUTP10 is an important protein in the processing of 18S rRNA.

1. Introduction

Ribosomes, large ribonucleoprotein complexes that perform protein synthesis, are essential for all living cells. The biogenesis of ribosomes is a very complex process that involves multistep pre-ribosomal RNA (pre-rRNA) cleavage and numerous modifications that are followed by the stepwise assembly of ribosomal proteins around completely processed rRNAs. The large ribosomal subunit (LSU or 60S) contains three rRNA molecules – 25/28S, 5.8S and 5S, while the small subunit (SSU or 40S) assembles around 18S rRNA. This process is very well studied and quite conserved throughout the eukaryotes [1,2].

Generally, ribosomes have a similar function in bacteria, archaea and eukaryotes. However, among these supergroups there are important differences in ribosome size, structure, composition and the rRNA:protein ratio [3]. Classically-shaped eukaryotic 80S ribosomes are composed of 60S LSU and 40S SSU, together containing more than 70 ribosomal proteins and 4 rRNAs. Processing of rRNAs and ribosome biosynthesis are carefully orchestrated processes that begin in the nucleolus, continue in the nucleoplasm and are completed in the cytoplasm [4].

The rRNA genes are organized in conserved repeated clusters, usually present in dozens to hundreds of copies. The precursor for 25S/28S, 18S and 5.8S rRNA is transcribed in the nucleolus by RNA polymerase I as a single 35S pre-rRNA transcript, while the precursor for 5S rRNA is generated by RNA polymerase III in the nucleoplasm. The 35S precursor, best studied in *Saccharomyces cerevisiae*, has an ETS/18S/ITS1/5.8S/ITS2/28S/ETS order, where ITS and ETS stand for the internal and external transcribed spacer, respectively. It is co-transcriptionally modified by multiple pseudouridylations and 2′-O-ribose methylations. The entire rRNA maturation process involves several small nucleolar (sno) RNAs, as well as many proteins including endo- and exonucleases operating in large complexes [5].

The late stages of SSU and LSU maturations are well understood, whereas we know relatively little about the early stages of 18S rRNA

* Corresponding authors at: Institute of Parasitology, Branišovská 31, 370 05 České Budějovice, Czech Republic.
E-mail address: dranov@paru.cas.cz (D. Faktorová).
[1] Present address: Kepler University, Linz, Austria.

https://doi.org/10.1016/j.molbiopara.2018.09.003
Received 18 July 2018; Received in revised form 28 August 2018; Accepted 15 September 2018
Available online 21 September 2018
0166-6851/

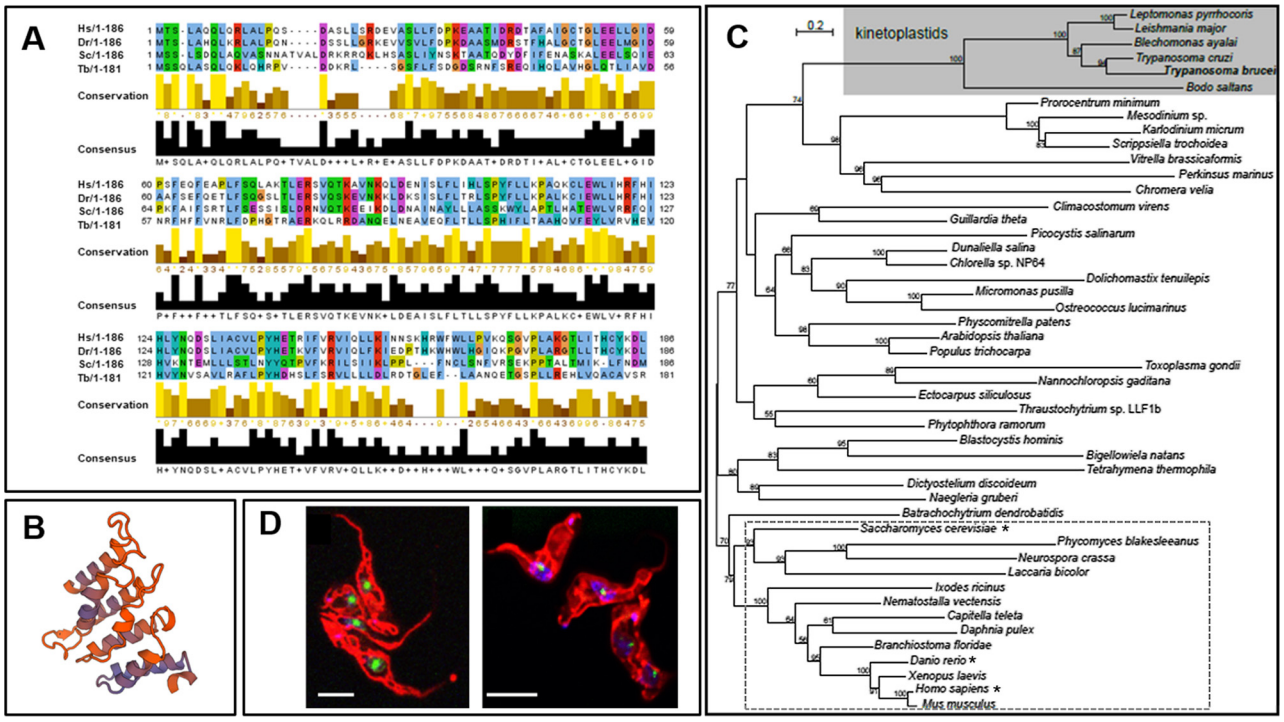

Fig. 1. *T. brucei* Tb927.9.2900 gene encodes a putative UTP10/Bap28/HEATR1 homolog.
A. Comparison of the N-terminus of TbUTP10 (Tb) and its homologs in zebrafish *Danio rerio* (Dr), human (Hs) and yeast *Saccharomyces cerevisiae* (Sc). The complete alignment is shown in Suppl. Fig. 1. **B.** Model of the TbUTP10 C-terminal HEAT domain built by SWISS MODEL using Centrosomal protein of 104 kDa as a template. **C**. Maximum likelihood topology of TbUTP10 eukaryotic homologues constructed using LG + F+R5 model as implemented in IQTree. Numbers at branches correspond to the ultrafast bootstrap branching support inferred from 50,000 replicates in IQTree. The dataset consisted of 48 taxa and 799 amino acid positions. See relevant part of Materials and Methods for details. Kinetoplastids are shown in grey box. The only three species of opisthokonts (dashed box) in which homologues of TbUTP10 were studied are indicated with a star. **D.** TbUTP10 protein is localized in the nucleolus of both PS (left) and BS (right) *T. brucei*. Localization of TbUTP10-Ty-GFP (in green) in the nucleolus. Mitochondria are stained in red (MitoTracker) and DNA in blue (Nuc Blue Live Cell Stain). Scale bar: 5 µm.

processing. This pathway initiates with the assembly of a large ribonucleoprotein (RNP) complex called the SSU processome, which is involved in the early-stage cleavage of the 18S rRNA transcript at positions A0, A1 and A2 [6,7]. The SSU processome is constituted of ribosome assembly factors UtpA, UtpB, UtpC and the U3 small nucleolar RNP [7]. The first subcomplex that associates with the pre-rRNA is the heptameric multi-protein UtpA complex, which includes UTP10 [8,9]. At the initiation of rRNA transcription, SSU processome subunits UTP8, UTP9 and UTP17 bind to the 5′ end of the nascent pre-rRNA, whereas UTP4, UTP5, UTP10 and UTP15 interact with nucleotides downstream of the 5′ ETS region. Furthermore, other UtpA and UtpB subunits bind to the 5′ ETS, subsequently recruiting the U3 snoRNP (formed by U3 snoRNA and Nop56, Nop58, Snu13, Nop1 and Rrp9 proteins), which also associates with the 5′ ETS. Finally, as transcription proceeds, the processome is assembled around a folded 18S rRNA [9–11]. Depletion of individual UtpA subunits hints at a role of this complex as the initiator of pre-ribosome assembly by binding to the nascent pre-rRNA and then recruiting UtpB and the U3 snoRNA [12]. Importantly, a subset of SSU processome components link RNA polymerase I transcription with pre-rRNA processing [13].

In the early diverging eukaryotic lineages represented almost invariably by protists, many fundamental cellular processes exhibit unusual features, with rRNA processing being no exception. *Trypanosoma brucei*, the causative agent of African sleeping sickness, is one such eukaryote belonging to the diverged supergroup Excavata [14] and the best studied representative of this clade. In this flagellate, the 28S rRNA is divided into two large LSUα and LSUβ fragments plus four small srRNA1-4 molecules, while its 18S rRNA is larger than in most other eukaryotes [15,16]. While the processing of pre-rRNA in yeast is initiated by cleavage of the 5´ ETS, in trypanosomes the processing initiates by the endonucleolytic separation of 18S rRNA from the rest of the precursor transcript [17]. Moreover, SSU processing is unique as two U3 snoRNA-crosslinkable 5′ ETS sites are required for SSU rRNA maturation in *T. brucei* [18–20].

Remarkably, about 140 snoRNAs were found in *T. brucei* to play a role in rRNA maturation, most of them being involved in modification, only about 20 in rRNA processing [21]. However, our knowledge of the protein factors participating in rRNA processing and ribosome biogenesis in *T. brucei* and other unicellular eukaryotes remains fragmentary at best and only several proteins have been studied so far. In particular, it was shown that the depletion of NOG1 or the LSU protein L5 lead to the accumulation of rRNA precursors and defect in 60S biogenesis [22,23]. On the other hand, the depletion of exoribonuclease XRNE leads to the accumulation of aberrant 18S and 5.8S rRNAs [24]. Finally, proteins TbNOB1 and TbPNO1 play a role in specific 18S rRNA 3′ end cleavage [25] and the U3 snoRNA-associated protein NOP1 was shown to be connected with trypanosome-specific rRNA processing events that generate small rRNA fragments. Interestingly, while silencing of NOP1 and NOP56 did not affect the level of snoRNAs, depletion of their partner NOP58 from the U3 snoRNP complex led to the destabilisation of several snoRNAs, including U3 [26]. The genome of *T. brucei* contains many other homologs of the processome factors [17], but no experimental data is available about the initial steps of its rRNA processing.

In this report, we have identified a homolog of the yeast UTP10 UtpA subunit, also known as BAP28 in zebrafish and HEATR1 in humans. We show that TbUTP10 is a nucleolar protein that is required for growth of procyclic (PS) and bloodstream stages (BS) of *T. brucei*, which infect the tsetse fly vector midgut and mammalian bloodstream, respectively. TbUTP10 is involved in the processing and maturation of pre-18S rRNA, its depletion resulting in U3 snoRNA depletion and an abnormal polysome profile, thus impairing ribosome assembly. These

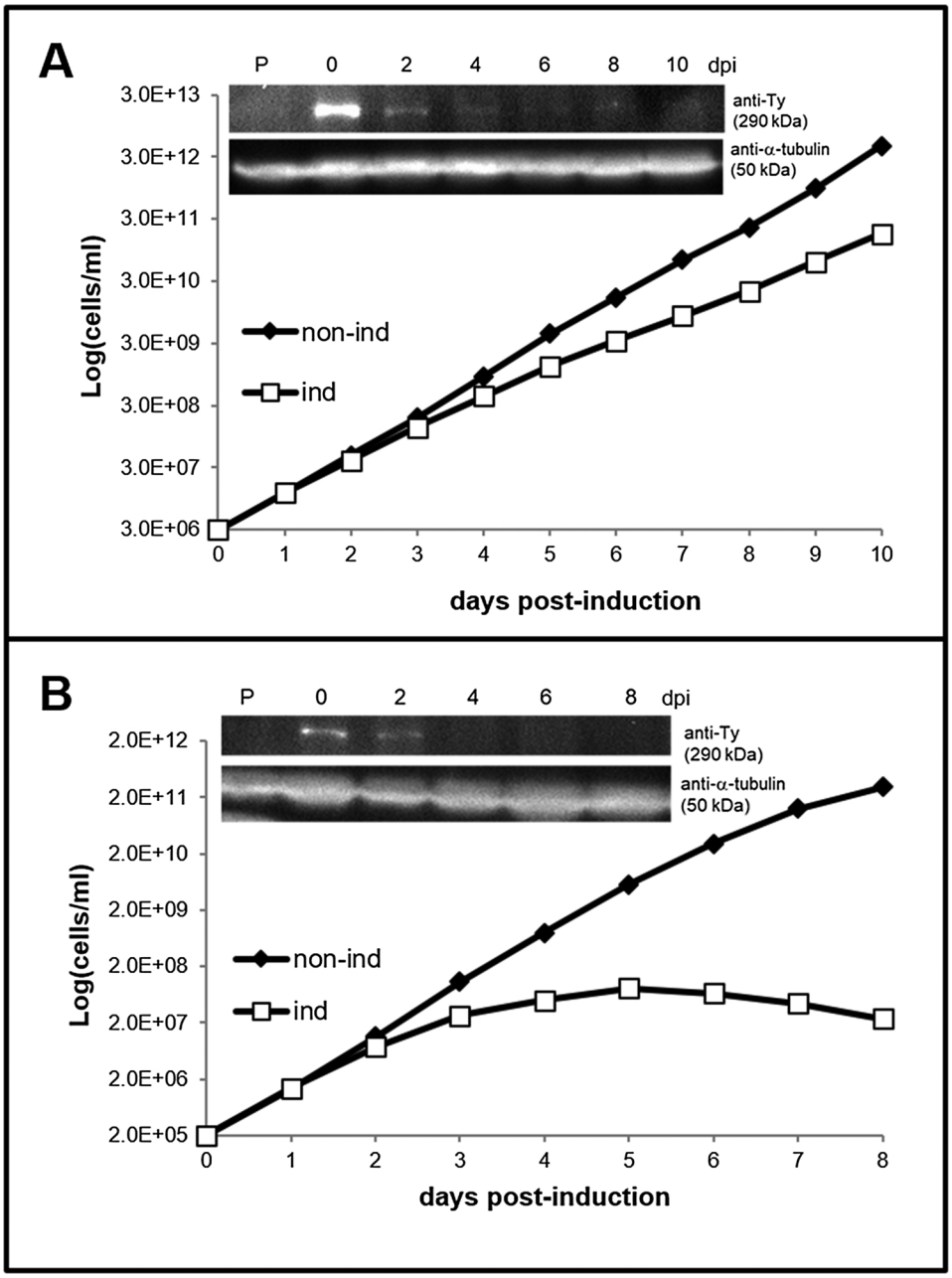

Fig. 2. TbUTP10 protein is essential for normal growth of both PS (left) and BS (right) *T. brucei*.
Cumulative growth curves of TbUTP10 RNAi (ind = RNAi induced with tetracycline) in PS cells (**A**) and BS cells (**B**) are shown, as compared to the non-induced controls (non-ind). Western blot analysis of TbUTP10-Ty-GFP levels during a RNAi time course in PS (**A** –inset) or BS (**B** - inset) probed with anti-Ty antibody; anti-α-tubulin antibody signal shown as a loading control. dpi, days post induction. Representative growth curves are shown, with the experiment repeated three times to ensure reproducibility.

results highlight a conserved role of TbUTP10 in the pre-18S rRNA maturation process of extremely evolutionary distant eukaryotes.

2. Results

2.1. Data mining and structural modelling reveal a putative T. brucei homolog of UTP10/BAP28/HEATR1

A structural homology search using HHpred [27] revealed the presence of a potential homolog of *UTP10/Bap28/HEATR1* in the *T. brucei* genome (Fig. 1A–C), annotated as Tb927.9.2900 in the TriTrypDB genome database [28], which we name *TbUTP10*. This homology is not readily apparent by overall sequence similarity (Suppl. Fig. 1). However, the N-terminus of the protein is highly conserved in comparison to UTP10 homologs from yeast, zebra fish and humans (Fig. 1A). The C-terminus of opisthokont UTP10 consists of a HEAT (Huntington, elongation A subunit, TOR) repeat, an iteration of two α-helices linked by a short loop [29]. The amino acid sequence similarity of the C-terminus of TbUTP10 with its putative opisthokont homologs is low (Suppl. Fig. 1), precluding determination if this motif is present in the trypanosomatid homolog. To overcome this problem, a Swiss-Model [30] prediction of the tertiary structure of the TbUTP10 C-terminus using the HEAT repeat of the 104 kDa centrosomal protein as a template was performed, indicating UTP10 ends with a HEAT repeat as in the other homologs (Fig. 1B).

TbUTP10 encodes a much larger protein (287 kDa) than its

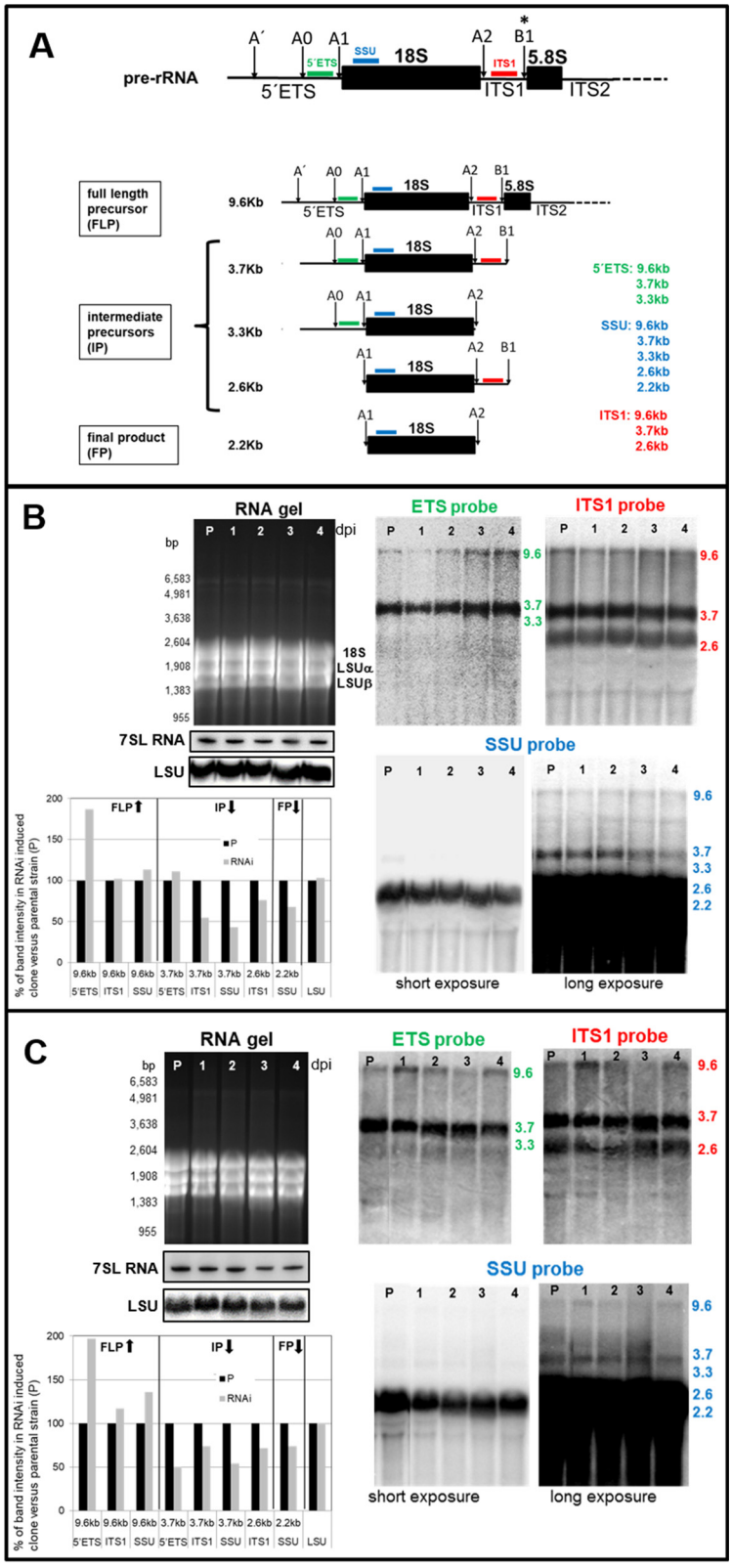

Fig. 3. TbUTP10 is involved in the processing of pre-18S rRNA.
A. First 18S rRNA processing steps in *T. brucei* (adapted from [17]). The asterisk shows the position of the first cleavage, B1 (top). Coloured bars indicate the positions of the 5′ ETS, SSU and ITS1 probes used for detection of the precursors in the pre-18S rRNA processing pathway. The respective lengths of full-length precursors (9.6 kb), intermediates (3.7 kb, 3.3 kb, 2.6 kb) and the final product (2.2 kb) (bottom) are also given. Please note that sizes are not to scale in this diagram. Northern blot analysis of parental strain (P) vs. PS TbUTP10 RNAi cells (**B**) and BS TbUTP10 RNAi cells (**C**), induced for 1 to 4 days (1 to 4). The colours in the panels correspond to the probes from Fig. 3A. The graphs show percentage of band intensity at a given control compared to the parental control of each RNA species depicted for both cell line: PS RNAi (**B**) and BS RNAi (**C**). 7SL rRNA was used as a normalized control, with the changes in RNA levels being calculated by normalisation of the wild type and RNAi-induced or sKO signal. A clear trend of accumulation of the full length precursors (FLP) and decrease of final products (FP) are shown by arrows, as well as the values for each intermediate product (IP). Representative Northern blots are shown, with the experiment repeated three times to ensure reproducibility.

opisthokont homologs in yeast (200 kDa), zebrafish (242 kDa) and human (236 kDa) [7,31,32]. The alignment of TbUTP10 with these sequences reveals several insertions that account for this increase in size (Suppl. Fig. 1). We checked all the extra sequences of *T. brucei* protein (which are mainly around 20 aa long, the longest one being 57 aa) using protein domains identifier – InterProScan (http://www.ebi.ac.uk/interpro/search/sequence-search), but didnt find any functional domains that might point to additional roles of this protein in *T. brucei* in comparison to orthologues in other systems.

Maximum likelihood-based phylogeny (Fig. 1C) of the UTP10 proteins recovered some of the main eukaryotic lineages, such as the opisthokonts, green algae including plants, dinoflagellates, chromerids, stramenopiles and kinetoplastids. It also revealed increased rates of evolution and high level of divergence in most clades, which results in a

low overall branching support especially in terminal branches. Kinetoplastids form a monophyletic and robustly supported group with internal branching corresponding to the accepted kinetoplastid phylogeny with *Bodo saltans* as a sister clade to the parasitic trypanosomatids (Fig. 1C).

2.2. TbUTP10 is localized in the nucleolus

In order to determine its localisation in the PS and BS *T. brucei*, the TbUTP10 gene was *in situ* C-terminally tagged with a tandem Ty epitope and enhanced yellow fluorescent protein (eYFP) tag. In both life cycle stages protein expression was high enough to record the signal directly in live cells. The advantage of live-cell imaging is that it avoids potential artefacts, which can be caused by fixation. In order to take pictures of moving trypanosomes after staining, we used a previously described technique, in which the cells are covered by a thin sheet of 1% agarose and directly observed by confocal microscopy [33]. TbUTP10 protein is localised in the nucleolus in both PS and BS cells (Fig. 1D). The individual channels are shown in Suppl. Fig. 5. This suggests that TbUTP10 function may be similar that of its opisthokont homologs.

2.3. Ablation of TbUTP10 severely affects fitness

T. brucei expressing the Ty-eYFP tagged TbUTP10 were electroporated with the p2T7-177 construct for tetracycline-inducible expression of a ~500 bp double stranded RNA targeting TbUTP10. The efficiency of RNAi was verified by Western blot analysis detecting TbUTP10-Ty-eYFP with an antibody recognizing the Ty epitope (Fig. 2A and B; insets). In both PS and BS *T. brucei*, a significant decrease of the tagged protein was observed after 2 days of RNAi induction, and it was almost undetectable after day 4.

Upon TbUTP10 depletion, growth inhibition was observed in both PS and BS RNAi-cell lines (Fig. 2A and B). However, this phenotype was more prominent in BS cells, where growth was already inhibited by day 2 after RNAi induction and then completely stopped after day 5, suggesting that TbUTP10 is an essential protein in this life stage. This hypothesis is further supported by the knock-out of a single *TbUTP10* allele (sKO) replaced with a hygromycin resistance marker (Suppl. Fig. 2A). Three independent attempts to prepare a *TbUTP10* double knock-out cell line failed, providing indirect evidence that the target protein is indeed essential.

2.4. TbUTP10 is directly involved in pre-18S rRNA processing

Since we hypothesized that TbUTP10 plays a role in 18S rRNA biosynthesis, we next investigated the impact of its depletion on pre-18S rRNA processing. More specifically, we predicted that ablation of TbUTP10 will cause the accumulation of pre-18S rRNA precursors, indicating an error in early stages of maturation.

Three different oligonucleotide probes (Table 4) were used in the Northern blot analysis. The position of these probes, as well as the sizes of all predicted precursors and the final product are depicted in Fig. 3A. The three cleavages at positions A0, A1, and A2 are required for the production of the mature 18S rRNA and consequently the 40S ribosomal subunit [17]. If TbUTP10 was involved in pre-18S rRNA processing, an increase of the 9.6 kb-long full-length precursor, and a concomitant decrease of the 2.2 kb-long final product was expected to occur upon TbUTP10 silencing. The intensities of the respective RNA species were quantified by densitometry and any changes (in percent) were calculated in comparison to RNA from control parental cell lines, 7SL RNA was used as a normalized control (Fig. 3B, C; Suppl. Fig. 2B and 3). The latter were chosen for comparison instead of uninduced RNAi cell lines to avoid any confounding effects of potential RNAi leakage.

The comparative analysis confirmed our hypothesis. On day 4 after RNAi induction of PS cells (Fig. 3B), the 5′ETS probe revealed a significant increase of the full-length precursor, as well as that of the 3.7 kb intermediate (we did not detect the 3.3 kb intermediate in our analysis). The increase of the 9.6 kb-long precursor and a parallel decrease of the smaller precursors was confirmed by the ITS1 probe. Finally, the SSU probe showed that the largest precursor accumulates, while the other RNA species bands decrease. The fully processed 2.2 kb-long product decreased by approximately 30% on day 4, meaning that production of the mature 18S rRNA is impaired. In contrast, signal of the LSU probe remained unaltered, showing that the defect in rRNA processing is only SSU specific.

The results obtained in the BS TbUTP10-RNAi cells are similar (Fig. 3C). All three probes showed an accumulation of the full-length precursor and a concomitant decrease of the 3.7 kb precursor upon the down-regulation of TbUTP10. The decrease of the mature 2.2 kb SSU rRNA product is less pronounced in the BS than in the PS cells, but the overall trend is the same. Moreover, the sKO cells showed an even more pronounced increase of the 9.6 kb-long 5′ETS precursor, with the ITS1 and SSU precursors also increased and the mature product decreased by about 20% (Suppl. Fig. 2B and 3). In conclusion, Northern blot analysis of full-length precursor and mature 18S rRNA upon ablation of TbUTP10 by two alternative approaches and in two different life cycle stages is consistent and shows that TbUTP10 is specifically involved in the 18S rRNA processing as it was already described in other organisms.

2.5. TbUTP10-depleted cells have an abnormal polysome profile

Since TbUTP10 is localised in the nucleolus and its depletion affects maturation of the pre-18S rRNA transcript, we next investigated whether its RNAi-mediated depletion results in an altered polysome profile, reflecting a defect in ribosome biogenesis. Based on the previously described processing phenotype, we predicted a decrease of the 40S SSU, which contains mature 18S rRNA, and a consequent decrease in the 80S ribosome. The amount of cells required for this experiment limited its application to the PS RNAi cell line. The lysates from parental cells and RNAi induced cell line were separated by 10 to 50% sucrose gradient centrifugation and the fractions were monitored by absorbance at 254 nm to detect the protein component of ribosomes (Fig. 4). Three biological replicates for each cell line had a very consistent pattern (Fig. 4A and B), allowing us to analyse their overlay using peak annotations (Fig. 4C).

The collective polysome profile of the TbUTP10-depleted *T. brucei* sample revealed that the 40S ribosomal subunit peak was completely missing. This was confirmed by hybridizing RNA isolated from individual fractions with SSU (18S) and LSU (28S) probes which showed a disappearance of the signal from fractions 3 and 4 corresponding to the 40S peak (Suppl. Fig. 4). Furthermore, it showed that the 60S subunit accumulated substantially, which may have been due to it not being incorporated into the 80S ribosome because of lack of availability of 40S subunits. This result is congruent with the 80S ribosome peak being much narrower than in the parental control. These results indicate that upon TbUTP10 down-regulation, the resulting 18S rRNA processing defect results in a decrease of the 40S SSU, ultimately impairing ribosomal assembly.

2.6. TbUTP10 silencing affects U3 snoRNA

As mentioned above, in yeast and other organisms UTP10 binds to U3 snoRNA and its associated proteins, thereby contributing to the maturation of 18S rRNA. Hence, we wondered whether the depletion of TbUTP10 will have an effect on the U3 snoRNA level. For that aim, the signal of U3 oligonucleotide probe was compared with the 7SL RNA signal, which was used as a loading control (Fig. 5). The intensities of the respective RNA species were quantified by densitometry and compared with RNA obtained from the control parental cell lines (Fig. 5A, B; Suppl. figure 2C and 3). Indeed, we observed a decrease of U3

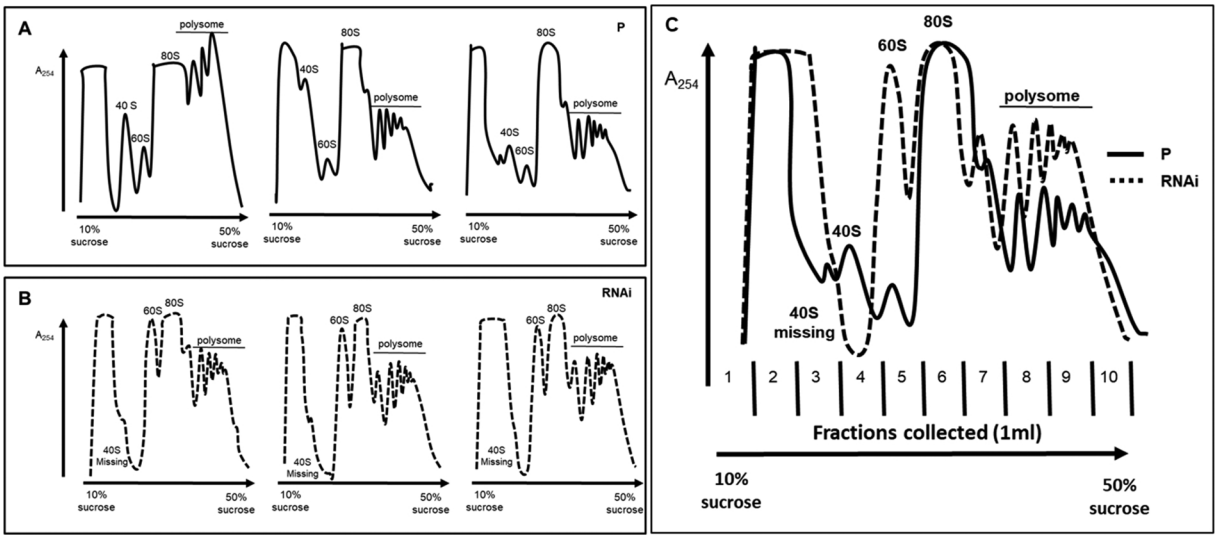

Fig. 4. Polysome profiling analysis of PS TbUTP10 RNAi cell line.
A. Parental PS cell line -P (solid black line); **B**. PS TbUTP10 RNAi cell line (dashed line). Peaks corresponding to 40S, 60S, 80S and the polysomes are indicated. **C**. Overlay of polysome profiling analysis of parental versus RNAi induced cells (the profiles to the right in panels A and B are compared as representative examples).

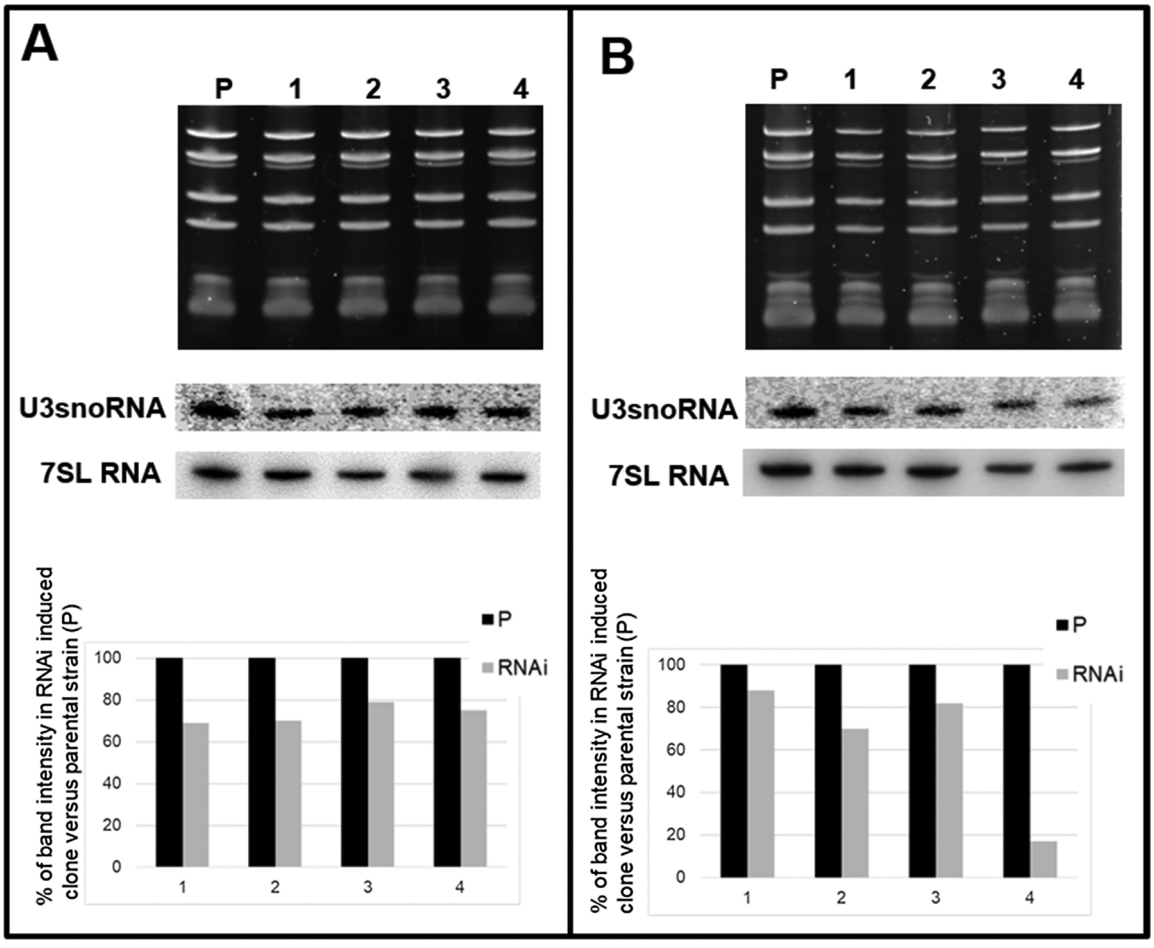

Fig. 5. TbUTP10-silencing affects U3 snoRNA.
Total RNA was separated on a denaturing 8% polyacrylamide/8 M urea gel (top) and Northern blot analysis of parental strain (P) vs. PS TbUTP10 RNAi cells (**A**) and BS TbUTP10 RNAi cells (**B**) induced for 1–4 days (I1 to I4) was performed. U3 oligonucleotide probe was compared to 7SL RNA.
The band intensity compared to the parental control of each rRNA species is depicted (in percentage) for both cell line: PS RNAi (**A**) and BS RNAi (**B**). 7SL RNA was used as a normalized control, with changes in the rRNA levels being calculated by normalisation of the wild type and the RNAi-induced signal to 7SL rRNA. Note the decrease of the level of U3 snoRNA in both TbUTP10-depleted cell line. Representative Northern blots are shown, with the experiment repeated three times to ensure reproducibility.

snoRNA level in each TbUTP10-depleted cell line.

3. Discussion

Ribosomes are crucial components of all cells, as they are responsible for translation of mRNAs into proteins. Their biosynthesis is a highly complex process that requires the action of numerous RNA and protein factors. Because of its ubiquity, this process is likely to be highly conserved, yet one would also expect lineage-specific novelties in highly divergent eukaryotes.

In agreement with this supposition, the ribosome of *T. brucei* has its share of unique features, which include its 28S rRNA split into 6 fragments [16] and the existence of unusual inter-subunit bridges, as observed by cryo-electron microscopy [34]. Furthermore, trypanosomatid 18S rRNA is very long compared to other organisms [15], with significant differences in pre-18S rRNA processing [17]. However, virtually nothing is known about the proteins mediating early stages of this process, motivating us to undertake functional analysis of TbUTP10, a protein known to be involved in 18S rRNA processing in opisthokonts [7,29,31]. Here, we have shown that the gene *Tb927.9.2900* in the excavate protist *T. brucei* is a distantly related homolog of yeast *UTP10*, zebrafish *BAP28* and human *HEATR1*, and therefore have renamed it *TbUTP10*. Due to its significant divergence from its opisthokont homologs, TbUTP10 had to be identified based on a tertiary structure prediction [27]. Interestingly, TbUTP10 is larger than its opisthokont homologs, which may be an adaptation to the longer length of its 18S rRNA substrate. We have shown that TbUTP10 is a nucleolar protein, which was also confirmed in the Tryptag protein localisation database for both N and C terminally tagged protein in PS stage (http://tryptag.org/?query=Tb927.9.2900). Northern analysis of knock-out and knock-down cell lines confirmed that it is involved in pre-18S rRNA processing. Although the band quantifications did not consistently exhibit the trend in all 18S rRNA intermediate precursors, there is a clear accumulation of full-length precursors and a decrease of the final 18S rRNA product. Combined, these results confirmed that UTP10 has a conserved function in excavates and opisthokonts.

Polysome analysis of TbUTP10-depleted PS trypanosomes revealed that the 40S SSU peak completely disappeared, which is consistent with the requirement of 18S rRNA for its maturation. The 60S LSU exhibited prominent accumulation, likely because it cannot be paired with the 40S SSU to form the 80S ribosome. Still, a residual amount of 40S SSU allowed the assembly of 80S ribosomes, albeit with reduced abundance. It is likely that this limited yet ongoing ribosomal assembly allowed continued proliferation of PS cells at a reduced growth rate. However, its dramatic impact on *T. brucei* BS growth and the profound change in the polysome profile of PS cells indicates an essential function of TbUTP10 in ribosome biogenesis. Additional evidence for the indispensability of TbUTP10 was a repeated failure to create a double knock-out cell line.

These observations are in agreement with biochemical studies performed in yeast and point to a conserved function. Association of UTP10 with pre-18S rRNA processing was first discovered in *S. cerevisiae*, where it co-purified with the SSU processome that specifically associated with the U3 snoRNA and also played a role in pre-rRNA transcription [7]. It was proposed that U3 snoRNP recruitment to the processome is enhanced by a UTP10-U3 snoRNA 3′ domain interaction [10]. Our results demonstrate that the depletion of TbUTP10 is associated with the decreased level of U3 snoRNA, which was also observed in cells down-regulated for Nop58, a protein that belongs to the U3snoRNP complex [26]. It is not an unexpected result, since recent structural studies revealed that these proteins actually seem to function next to each other [9,35,36]. Indeed, UTP10 deletion inhibited the early pre-rRNA processing steps in the 18S rRNA maturation, causing the accumulation of its precursors, although it had only mild effects on rRNA transcription and 25S or 5.8S rRNA synthesis. Depletion of Bap28 and HEATR1 in zebrafish and mammals, respectively, results in increased p53-dependent apoptosis in the central nervous system, leading to abnormal brain and organ development and subsequent death of zebrafish embryos [29,31].

In *T. brucei*, the essentiality of this protein (labelled under previous name Tb09.160.1560) was already indicated in the genome wide RNAi screen for all studied libraries - bloodstreams, procyclics as well as differentiated ones [37]. The growth defect following its depletion was more pronounced when TbUTP10 was depleted in BS. We speculate that this life cycle stage requires a more rapid flux of ribosome biogenesis due to faster proliferation of BS compared to PS. This hypothesis would agree with observation of increased HEATR1 levels in certain cancer types, which are also highly proliferative [38]. Taken together, our study showed that TbUTP10 has a conserved function in eukaryotes. Its importance for rapidly proliferating BS possibly parallels the effects of upregulation of HEATR1 in cancer cells.

4. Materials and methods

4.1. Phylogenetic analysis

Eukaryotic homologues of yeast UTP10 were identified using BLAST against the custom database with the representative sampling of eukaryotic lineages as well as HHPred in case of *T. brucei*. The dataset was aligned using E-INS-i algorithm implemented in MAFFT 7 [39], the ambiguously aligned and/or gap-rich regions were manually extracted using SeaView 4 [40]. The resulting dataset contained 48 taxa and 799 amino acid positions. The phylogeny of UTP10 was inferred using Maximum likelihood under the LG + F+R5 model (5 categories of variable sites with relaxed distribution) as implemented in IQTree 1.5 [41]. This particular model was chosen as the best fitting based on AIC and BIC scores in a modeltest implemented in IQTree. Ultra-fast bootstrap values as a mean of branching support were assessed from 50,000 replications.

4.2. T. brucei cell lines, cultivation and growth curves

T. brucei PS SMOXP9 strain [42] was grown at 27 °C in SDM-79 medium [43] supplemented with 10% fetal bovine serum (FBS), while BS 427 - single marker strain [44] was kept at 37 °C and 5% CO_2 in HMI-9 medium supplemented with 10% FBS. Additionally, antibiotics were added to the media according to the selection markers present (Tables 1 and 2). For growth measurements, BS and PS cells were induced at a density of 2×10^5/ml and 3×10^6/ml, respectively, counted daily using a Z2 Particle Counter (Beckman Coulter) and diluted back to the initial density as appropriate. Representative growth curves are shown, with the experiment repeated three times to ensure reproducibility.

4.3. Generation of cell lines

4.3.1. Generation of cell lines expressing tagged TbUTP10

In PS cells, TbUTP10 was endogenously C-terminally tagged with a tandem Ty epitope and eYFP tag using recently developed tagging tools for trypanosomes [45]. The pPOTv2 vector was a template for PCR with

Table 1
Antibiotics mixture compositions for different cell lines.

Used T. brucei strains	Added antibiotics
PS wt (SMOX P9)	Puromycin
PS TbUTP10 YFP + Ty tagged RNAi cell line (clone 4)	Puromycin, Hygromycin, Phleomycin
BS wt (427)	G418
BS TbUTP10 YFP + Ty tagged RNAi cell line (clone 2)	G418, Hygromycin, Phleomycin
BS sKO-Hygro	G418, Hygromycin

Table 2
Concentrations of all antibiotics in respective media.

	Concentrations in medium	
Used antibiotics	PS	BS
G418	–	2.5 μg/ml
Puromycin	0.5 μg/ml	
Phleomycin	2.5 μg/ml	2.5 μg/ml
Hygromycin	25 μg/ml	2 μg/ml
Tetracycline (for RNAi inductions only)	1 μg/ml	1 μg/ml

~100 bp primers (2900_Ty_Fwd and 2900_Ty_Rev; see Table 3 for all primer sequences), of which the 5′-most 80 bp represented homologous flanks for recombination into the *TbUTP10* locus. The PCR product that was directly electroporated into SMOXP9 cell line, and clones were selected using hygromycin.

In BS cells, three attempts of this rapid technique failed. Therefore, we decided to extend the flanking homologous regions to about 500 bp and performed a separate amplification of the left (primers A-5U2900-F and A-5U2900-YFP-R primers) and right (primers B-3U2900-Hyg-F and B-3U2900-R) homology arms, plus the Ty + eYFP tags and hygromycin^R cassette from the pPOTv2 vector (primers C-YFP_Hyg-F and C-YFP_Hyg-R). These PCR products were fused into a final product (primers D-Nest-2900-F and D-Nest-2900-R), which was purified and subsequently electroporated into BS 427 cells.

4.3.2. Generation of RNAi and single knock-out cell lines

A 515 bp fragment of the TbUTP10 gene was PCR amplified from genomic DNA (primers 2900_p2T7_Fw and 2900_p2T7_Rv) and cloned into the p2T7-177 vector [46] via the XhoI and BamHI restriction sites. The linearized p2T7-177 vector was subsequently electroporated into both tagged cell lines and clones were selected with phleomycin. PS cell and BS cell clones were induced with 1 μg/ml tetracycline. Single knock-out of TbUTP10 in the BS 427 strain was generated using the fusion PCR method [47], with the hygromycin resistance marker cassette flanked by TbUTP10′s 5′- and 3′-untranslated regions to facilitate homologous recombination. These constructs were sequentially electroporated into the cells.

Table 4
DNA oligonucleotide probes used for Northern blot hybridization.

Probe	Sequence of the probe
5'ETS	5'-AGTGTAAGCGCGTGATCCGCTGT-3'
SSU	5'-GGCTAAGTCCTTGAAACAAGCA-3'
ITS1	5'-GGTTGCATACTGTGCAATTATACATGC-3'
LSU	5'-GTCCTGCCACACTCAGGTCTGA-3'
U3 snoRNA	5´-TGC CGT TCA TCG AAC-3`
7SL RNA	5´-CAACACCGACACGCAACC-3`

4.4. Localisation of TbUTP10 protein in live cells

In order to visualize TbUTP10, 5×10^6 live PS or BS cells were stained with 1 μl of 20 μM MitoTracker Red CMXRos (Molecular Probes) and two drops of Nuc Blue Live Cell Stain (Molecular Probes), incubated for 15 min at their respective cultivation conditions, spun down and resuspended in Iscove's Modified Dulbecco's Medium. The cells were subsequently immobilized under a sheet of 1% agarose and observed under an OlympusFluoViewFV1000 confocal microscope as described elsewhere [33].

4.5. Western blot analysis

Cell lysates were prepared in Laemmli sample buffer at a concentration allowing the loading of 5×10^6 cells per lane and separated on a 3-10% gradient SDS-PAGE gel. The proteins were subsequently transferred onto a PVDF membrane by electro-blotting at 20 V overnight to ensure transfer of large molecular weight proteins. Membranes were blocked with 5% (w/v) non-fat milk prepared in PBS with 0.5% (v/v) Tween 20 and probed with monoclonal mouse α-Ty antibody (1:2000; Sigma Aldrich) overnight at 4 °C. The membrane was subsequently incubated with secondary α-mouse polyclonal antibody conjugated with horseradish peroxidase (1:1000) (Sigma) and visualized using Clarity western ECL substrate (Bio-Rad). Monoclonal anti-α-tubulin antibody produced in mouse (1:1000; Sigma T9026) was used as a loading control.

Table 3
DNA oligonucleotides used as PCR primers.

Primers	Sequence
Procyclic tagging	
2900_Ty_Fwd	TCGTTGTGGAGCAGGCGCGGAGGTTGTGTGGACATCTTTCATCCATTACGGGCCAAGATGTCCTGTATGCGATGGGTTCCACTAGTGTGAGCAAGG
2900_Ty_Rev	TCTTGACTTAGAGAGCTACCTCACCGAGATGTCATCGTGTACATGTACTCCAAGGCACACCCTTCCCATTGCAGCGGGTACTATTCCTTTGCCCTCGGAC
Bloodstream tagging	
A-5U2900-F	CATGCGGCAGATCTCATAGC
A-5U2900-YFP-R	ACTAGTGTGAGCAAGGGGAACCCATCGCATACAGG
B-3U2900-Hyg-F	GTCCGAGGGCAAAGGAATAGTACCCGCTGCAATGGGAAGGG
B-3U2900-R	GAGAAAAATAAAGAAGGGA
C-YFP_Hyg-F	ACTAGTGTGAGCAAGGGCGAG
C-YFP_Hyg-R	CTATTCCTTTGCCCTCGGAC
D-Nest-2900-F	GCTCAACAGCATCAGGATCA
D-Nest-2900-R	CACCAACACCACATCTGTCAA
RNAi primers	
2900_p2T7_Fw	CGACTCGAGACATGGCGCGTACTTTTACC
2900_p2T7_Rv	CGAGGATCCAGACAGTCACGCAACAGCAC
Bloodstream knock-out	
A-5U2900-F	CCCCCTACACTGTTCACACC
A-5U2900-Hyg-R	GGTGAGTTCAGGCTTTTTCATTTGCTCAAGCAGTTACTTA
B-3U2900-Hyg-F	GTCCGAGGGCAAAGGAATAGTACCCGCTGCAATGGGAAGG
B-3U2900-R	ACCAAAACCTTTGTCCCTCA
C-Hyg-F	ATGAAAAAGCCTGAACTCACC
C-Hyg-R	CTATTCCTTTGCCCTCGGAC
D-Nest-2900-F	TGCAGGCTCCCTACTACAGC
D-Nest-2900-R	AAGAGGGGGAAAAGGTAGCA

4.6. Northern blot analysis

Total RNA was isolated using TriReagent (MRC), precipitated, and resuspended in RNase-free water. For the analysis of small rRNAs, 5 µg of total cellular RNA was separated on a denaturing 8% polyacrylamide/8 M urea gel, electroblotted to Zeta-Probe membrane and cross-linked to the membrane with UV light. For the analysis of bigger rRNAs, 10 µg were loaded on a 1% agarose-formaldehyde gel. Samples were blotted overnight to a Zeta-Probe membrane by capillarity action and subsequently UV cross-linked as described previously [48]. The probes (Table 4) were radiolabelled with [γ^{32} P] dATP using polynucleotide kinase (New England Biolabs) and hybridization with the probe was performed overnight at 45 °C (U3 snoRNA and 7SL RNA probes) or 50 °C (the other probes). The membrane was exposed to a Fuji Imaging phosphor screen and scanned in a Phoshoimager (Amersham) for signal detection.

4.7. Sucrose density gradient sedimentation

The polysome profile analysis was performed as described previously [49]. Fifty mL shaking cultures were grown overnight at 27 °C to mid-log phase. Cells were collected by centrifugation and all subsequent steps were carried out at 4 °C. Cells were washed twice in 15 mL of ice-cold PBS supplemented with 100 µg/mL cyclohexamide and final pellet suspended in 780 µl of polysome buffer (10 mM Tris-HCl pH 7.5, 300 mM KCl, 10 mM MgCl2) supplemented with 100 µg/mL cyclohexamide, 2 mM DTT, and 1X Protease inhibitor cocktail. Cells were lysed by addition of NP-40 to a final concentration of 0.25% and incubated on ice for 10 min. Lysates were clarified by centrifugation at 15,000 g for 10 min. One mg equivalent of OD260 units was loaded on each 10–50% sucrose gradient prepared in lysis buffer and centrifuged at 36,600 RPM for 2 h at 4 °C in a Beckman SW41Ti rotor. A gradient fractionator (ISCO UA-6 UV Vis with Type 11 optical unit) was used to record UV profiles.

Conflict of interest

Authors have no conflict of interest to declare.

Acknowledgements

We thank Keith Gull and Sam Dean (University of Oxford) for providing the pPOTv2 plasmid, Moritz Niemann (Universität Bern) for advice on using the HHpred database and Zhenqui Huang (Arizona State University) for help with the cell immobilisation technique. Support from the Czech Grant Agency (16-18699S to JL and 17-24036S to HH), ERCCZ LL1601 and the ERD Funds, project OPVVV 16_019/0000759 are kindly acknowledged.

Appendix A. Supplementary data

Supplementary material related to this article can be found, in the online version, at doi:https://doi.org/10.1016/j.molbiopara.2018.09.003.

References

[1] S. Klinge, F. Voigts-Hoffmann, M. Leibundgut, N. Ban, Atomic structures of the ribosome, 2018eukaryotic ribosome, Trends Biochem. Sci. 37 (2012) 189–198.
[2] D.N. Wilson, J.H. Doudna Cate, The structure and function of the eukaryotic ribosome, Cold Spring Harb. Perspect. Biol. (2012) 4.
[3] S. Melnikov, A. Ben-Shem, N. Garreau de Loubresse, L. Jenner, G. Yusupova, M. Yusupov, One core, two shells: bacterial and eukaryotic ribosomes, Nat. Struct. Mol. Biol. 19 (2012) 560–567.
[4] H. Tschochner, E. Hurt, Pre-ribosomes on the road from the nucleolus to the cytoplasm, Trends Cell Biol. 13 (2003) 255–263.
[5] J. Venema, D. Tollervey, Ribosome synthesis in *Saccharomyces cerevisiae*, Ann. Rev. Genet. 33 (1999) 261–311.
[6] K.A. Bernstein, E.G. Gallagher Jennifer, B.M. Mitchell, S. Granneman, S.J. Baserga, The small-subunit processome is a ribosome assembly intermediate, Eukaryot. Cell 3 (2004) 1619–1626.
[7] F. Dragon, J.E. Gallagher, P.A. Compagnone-Post, B.M. Mitchell, K.A. Porwancher, K.A. Wehner, S. Wormsley, R.E. Settlage, J. Shabanowitz, Y. Osheim, A.L. Beyer, D.F. Hunt, S.J. Baserga, A large nucleolar U3 ribonucleoprotein required for 18S ribosomal RNA biogenesis, Nature 417 (2002) 967–970.
[8] G. Pöll, S. Li, U. Ohmayer, T. Hierlmeier, P. Milkereit, J. Perez-Fernandez, *In vitro* reconstitution of yeast tUTP/UTP A and UTP B subcomplexes provides new insights into their modular architecture, PLoS One 9 (2014) e114898.
[9] Q. Sun, X. Zhu, J. Qi, W. An, P. Lan, D. Tan, R. Chen, B. Wang, S. Zheng, C. Zhang, X. Chen, W. Zhang, J. Chen, M.Q. Dong, K. Ye, Molecular architecture of the 90S small subunit pre-ribosome, eLife 6 (2017) e22086.
[10] M. Hunziker, J. Barandun, E. Petfalski, D. Tan, C. Delan-Forino, K.R. Molloy, K.H. Kim, H. Dunn-Davies, Y. Shi, M. Chaker-Margot, B.T. Chait, T. Walz, D. Tollervey, S. Klinge, UtpA and UtpB chaperone nascent pre-ribosomal RNA and U3 snoRNA to initiate eukaryotic ribosome assembly, Nat. Commun. 7 (2016) 12090.
[11] M. Chaker-Margot, Assembly of the small ribosomal subunit in yeast: mechanism and regulation, 2018 regulation, RNA 24 (2018) 881–891.
[12] J. Pérez-Fernández, A. Román, J. De Las Rivas, X.R. Bustelo, M. Dosil, The 90S preribosome is a multimodular structure that is assembled through a hierarchical mechanism, Mol. Cell. Biol. 27 (2007) 5414–5429.
[13] J.E. Gallagher, D.A. Dunbar, S. Granneman, B.M. Mitchell, Y. Osheim, A.L. Beyer, S.J. Baserga, RNA polymerase I transcription and pre-rRNA processing are linked by specific SSU processome components, Genes Dev. 18 (2004) 2506–2517.
[14] V. Hampl, L. Hug, J.W. Leigh, J.B. Dacks, B.F. Lang, A.G. Simpson, A.J. Roger, Phylogenomic analyses support the monophyly of Excavata and resolve relationships among eukaryotic "supergroups, Proc. Natl. Acad. Sci. U. S. A. 106 (2009) 3859–3864.
[15] D.A. Campbell, K. Kubo, C.G. Clark, J.C. Boothroyd, Precise identification of cleavage sites involved in the unusual processing of trypanosome ribosomal RNA, J. Mol. Biol. 196 (1987) 113–124.
[16] T.C. White, G. Rudenko, P. Borst, Three small RNAs within the 10 kb trypanosome rRNA transcription unit are analogous to Domain VII of other eukaryotic 28S rRNAs, Nucleic Acids Res. 14 (1986) 9471–9489.
[17] S. Michaeli, rRNA biogenesis in trypanosomes, in: A. Bindereif (Ed.), Nucleic Acids and Molecular Biology, vol. 28, 2011, pp. 123–148.
[18] T. Hartshorne, Distinct regions of U3 snoRNA interact at two sites within the 5´external transcribed spacer of pre-rRNAs in *Trypanosoma brucei* cells, Nucleic Acids Res. 26 (1998) 2541–2553.
[19] T. Hartshorne, W. Toyofuku, Two 5-ETS regions implicated in interactions with U3 snoRNA are required for small subunit rRNA maturation in *Trypanosoma brucei*, Nucl. Acids Res. 27 (1999) 3300–3309.
[20] T. Hartshorne, W. Toyofuku, J. Hollenbaugh, *Trypanosoma brucei* 5'ETS A'-cleavage is directed by 3'-adjacent sequences, but not two U3 snoRNA-binding elements, which are all required for subsequent pre-small subunit rRNA processing events, J. Mol. Biol. 313 (2001) 733–749.
[21] S.K. Gupta, A. Hury, Y. Ziporen, H. Shi, E. Ullu, S. Michaeli, Small nucleolar RNA interference in *Trypanosoma brucei*: mechanism and utilization for elucidating the function of snoRNAs, Nucleic Acids Res. 38 (2010) 7236–7247.
[22] B.C. Jensen, Q. Wang, C.T. Kifer, M. Parsons, The NOG1 GTP-binding protein is required for biogenesis of the 60 S ribosomal subunit, J. Biol. Chem. 278 (2003) 32204–32211.
[23] K. Umaer, M. Ciganda, N. Williams, Ribosome biogenesis in African trypanosomes requires conserved and trypanosome-specific factors, Eukaryot. Cell 13 (2014) 727–737.
[24] J. Sakyiama, S.L. Zimmer, M. Ciganda, N. Williams, L.K. Read, Ribosome biogenesis requires a highly diverged XRN family 5'-&3' exoribonuclease for rRNA processing in *Trypanosoma brucei*, RNA 19 (2013) 1419–1431.
[25] S. Kala, V. Mehta, C.W. Yip, H. Moshiri, H.S. Najafabadi, R. Ma, N. Nikpour, S.L. Zimmer, R. Salavati, The interaction of a *Trypanosoma brucei* KH-domain protein with a ribonuclease is implicated in ribosome processing, Mol. Biochem. Parasitol. 211 (2017) 94–103.
[26] S. Barth, B. Shalem, A. Hury, I.D. Tkacz, X.H. Liang, S. Uliel, I. Myslyuk, T. Doniger, M. Salmon-Divon, R. Unger, S. Michaeli, Elucidating the role of C/D snoRNA in rRNA processing and modification in *Trypanosoma brucei*, Eukaryot. Cell 7 (2008) 86–101.
[27] J. Söding, A. Biegert, A.N. Lupas, The HHpred interactive server for protein homology detection and structure prediction, Nucleic Acids Res. 33 (2005) W244–248.
[28] M. Aslett, C. Aurrecoechea, M. Berriman, J. Brestelli, B.P. Brunk, M. Carrington, D.P. Depledge, S. Fischer, B. Gajria, X. Gao, M.J. Gardner, A. Gingle, G. Grant, O.S. Harb, M. Heiges, C. Hertz-Fowler, R. Houston, F. Innamorato, J. Iodice, J.C. Kissinger, E. Kraemer, W. Li, F.J. Logan, J.A. Miller, S. Mitra, P.J. Myler, V. Nayak, C. Pennington, I. Phan, D.F. Pinney, G. Ramasamy, M.B. Rogers, D.S. Roos, C. Ross, D. Sivam, D.F. Smith, G. Srinivasamoorthy, C.J. Stoeckert Jr, S. Subramanian, R. Thibodeau, A. Tivey, C. Treatman, G. Velarde, H. Wang, TriTrypDB: a functional genomic resource for the Trypanosomatidae, Nucleic Acids Res. 38 (2009) D457–462.
[29] Z. Turi, M. Senkyrikova, M. Mistrik, J. Bartek, P. Moudry, Perturbation of RNA polymerase I transcription machinery by ablation of HEATR1 triggers the RPL5/RPL11-MDM2-p53 ribosome biogenesis stress checkpoint pathway in human cells, Cell Cycle 17 (2018) 92–101.
[30] M. Biasini, S. Bienert, A. Waterhouse, K. Arnold, G. Studer, T. Schmidt, F. Kiefer, T. Gallo Cassarino, M. Bertoni, L. Bordoli, T. Schwede, SWISS-MODEL: modelling

protein tertiary and quaternary structure using evolutionary information, Nucleic Acids Res. 42 (2014) W252–258.
[31] M. Azuma, R. Toyama, E. Laver, I.B. Dawid, Perturbation of rRNA Synthesis in the bap28 Mutation leads to apoptosis mediated by p53 in the zebrafish central nervous system, J. Biol. Chem. 281 (2006) 13309–13316.
[32] J.L. Prieto, B. McStay, Recruitment of factors linking transcription and processing of pre-rRNA to NOR chromatin is UBF-dependent and occurs independent of transcription in human cells, Genes Dev. 21 (2007) 2041–2054.
[33] Z. Huang, S. Kaltenbrunner, E. Šimková, D. Staněk, J. Lukeš, H. Hashimi, Dynamics of mitochondrial RNA-binding protein complex in *Trypanosoma brucei* and its petite mutant under optimized immobilization conditions, Eukaryot. Cell 13 (2014) 1232–1240.
[34] Y. Hashem, A. des Georges, J. Fu, S.N. Buss, F. Jossinet, A. Jobe, Q. Zhang, H.Y. Liao, R.A. Grassucci, C. Bajaj, E. Westhof, S. Madison-Antenucci, J. Frank, High-resolution cryo-electron microscopy structure of the *Trypanosoma brucei* ribosome, Nature 494 (2013) 385–389.
[35] M. Kornprobst, M. Turk, N. Kellner, J. Cheng, D. Flemming, I. Koš-Braun, M. Koš, M. Thoms, O. Berninghausen, R. Beckmann, E. Hurt, Architecture of the 90S preribosome: a structural view on the birth of the eukaryotic ribosome, Cell 166 (2016) 380–393.
[36] J. Barandun, M. Chaker-Margot, M. Hunziker, K.R. Molloy, B.T. Chait, S. Klinge, The complete structure of the small-subunit processome, Nat. Struct. Mol. Biol. 24 (2017) 944–953.
[37] S. Alsford, D.J. Turner, S.O. Obado, A. Sanchez-Flores, L. Glover, M. Berriman, C. Hertz-Fowler, D. Horn, High-throughput phenotyping using parallel sequencing of RNA interference targets in the African trypanosome, Genome Res. 21 (2011) 915–924.
[38] Z.B. Wu, C. Qiu, A.L. Zhang, L. Cai, S.J. Lin, Y. Yao, Q.S. Tang, M. Xu, W. Hua, Y.W. Chu, Y. Mao, J.H. Zhu, J. Xu, L.F. Zhou, Glioma-associated antigen HEATR1 induces functional cytotoxic T lymphocytes in patients with glioma, J. Immunol. Res. (2014) 131494.
[39] K. Katoh, D.M. Standley, MAFFT multiple sequence alignment software version 7: improvements in performance and usability, Mol. Biol. Evol. 30 (2013) 772–780.
[40] M. Gouy, S. Guindon, O. Gascuel, SeaView version 4: a multiplatform graphical user interface for sequence alignment and phylogenetic tree building, Mol. Biol. Evol. 27 (2010) 221–224.
[41] L.T. Nguyen, H.A. Schmidt, A. Von Haeseler, B.Q. Minh, IQ-TREE: a fast and effective stochastic algorithm for estimating maximum-likelihood phylogenies, Mol. Biol. Evol. 32 (2015) 268–274.
[42] S.K. Poon, L. Peacock, W. Gibson, K. Gull, S. Kelly, A modular and optimized single marker system for generating *Trypanosoma brucei* cell lines expressing T7 RNA polymerase and the tetracycline repressor, Open Biol. 2 (2012) 110037.
[43] R. Brun, M. Schönenberger, Cultivation and in vitro cloning or procyclic culture forms of *Trypanosoma brucei* in a semi-defined medium. Short communication, Acta Trop. 36 (1979) 289–292.
[44] E. Wirtz, S. Leal, C. Ochatt, G.A. Cross, A tightly regulated inducible expression system for conditional gene knock-outs and dominant-negative genetics in *Trypanosoma brucei*, Mol. Biochem. Parasitol. 99 (1999) 89–101.
[45] S. Dean, J.D. Sunter, J. Wheeler Richard, I. Hodkinson, E. Gluenz, K. Gull, A toolkit enabling efficient, scalable and reproducible gene tagging in trypanosomatids, Open Biol. 5 (2015) 140197.
[46] B. Wickstead, K. Ersfeld, K. Gull, Targeting of a tetracycline-inducible expression system to the transcriptionally silent minichromosomes of *Trypanosoma brucei*, Mol. Biochem. Parasitol. 125 (2002) 211–216.
[47] C. Merritt, K. Stuart, Identification of essential and non-essential protein kinases by a fusion PCR method for efficient production of transgenic *Trypanosoma brucei*, Mol. Biochem. Parasitol. 190 (2013) 44–49.
[48] E. Vondrušková, J. van den Burg, A. Zíková, N.L. Ernst, K. Stuart, R. Benne, J. Lukeš, RNA interference analyses suggest a transcript-specific regulatory role for mitochondrial RNA-binding proteins MRP1 and MRP2 in RNA editing and other RNA processing in *Trypanosoma brucei*, J. Biol. Chem. 280 (2005) 2429–2438.
[49] I.M. Fleming, Z. Paris, K.W. Gaston, R. Balakrishnan, K. Fredrick, M.A. Rubio, J.D. Alfonzo, A tRNA methyltransferase paralog is important for ribosome stability and cell division in *Trypanosoma brucei*, Sci. Rep. 6 (2016) 21438.